ASEAN
Journal of Scientific and Technological Reports
Online ISSN:2773-8752

Research article

X-ray Shielding Properties of Natural Rubber/$BaSO_4$ Foam Composites

Narit Klompong[1], Arnon Srisook[2], Pornpana Buaphet[3], Suwit Phethuayluk[4], and Sutthisa Konruang[5*]

[1] Faculty of Science and Fisheries Technology, Rajamangala University of Technology Srivijaya, Trang, 92150, Thailand
[2] Regional Medical Sciences Center 11 Suratthani, 84100, Thailand
[3] Faculty of Science and Digital Innovation0, Thaksin University, Phatthalung, 93210, Thailand
[4] Faculty of Science and Digital Innovation0, Thaksin University, Phatthalung, 93210, Thailand
[5] Faculty of Science and Digital Innovation0, Thaksin University, Phatthalung, 93210, Thailand
* Correspondence: e-mail@e-mail.com; sutthisa@tsu.ac.th

Citation:
Klompong, N.; Srisook, A.; Buaphet, P.; Phethuayluk, S.; Konruang, S. X-ray shielding properties of natural rubber/$BaSO_4$ Foam composites. *ASEAN J. Sci. Tech. Report.* **2025**, *28*(3), e256422. https://doi.org/10.55164/ajstr.v28i3.256422.

Article history:
Received: October 22, 2024
Revised: March 22, 2025
Accepted: March 29, 2025
Available online: April 26, 2025

Abstract: In this study, lead-free X-ray shielding materials were fabricated using natural rubber (NR) and barium sulfate ($BaSO_4$) with various $BaSO_4$ filler loadings of 0, 50, 75, and 100 phr. The X-ray shielding properties of NR/$BaSO_4$ foam composites were investigated at X-ray tube voltages of 60, 70, 80, and 90 kVp. The results showed that the X-ray attenuation efficiency increased with higher $BaSO_4$ filler content and material thickness but slightly decreased with increasing voltages. The X-ray radiation attenuation properties were analyzed using the linear attenuation coefficient (μ_l) and the mass attenuation coefficient (μ_m). The results indicated that both coefficients increased with higher $BaSO_4$ filler content but decreased as the voltage increased. In contrast, the half-value layer (HVL) decreased with increasing $BaSO_4$ filler content but increased with higher voltages. In conclusion, NR/$BaSO_4$ foam composites have great potential for developing flexible and environmentally friendly X-ray shielding materials.

Keywords: Natural rubber foam; Barium sulfate; X-ray shielding

1. Introduction

X-rays are widely used in various industries, including nuclear reactors, airports, agriculture, and medical fields [1-2]. However, overexposure to X-ray radiation can negatively affect users, causing symptoms such as nausea, vomiting, fatigue, diarrhea, headaches, skin burns, and, in severe cases, death [3]. Therefore, it is necessary to develop radiation shielding materials to attenuate and prevent harmful X-ray exposure. Lead (Pb) is the most commonly used material for radiation shielding due to its high atomic number (82), which enables it to absorb radiation efficiently [1]. However, lead is a toxic material that poses significant health and environmental hazards [2]. Additionally, lead is heavy and non-flexible, making it inconvenient for users [4]. As a result, researchers have been exploring alternative materials for X-ray shielding, such as iron oxide (Fe_2O_3) [5], tungsten oxide (WO_3) [6], bismuth oxide (Bi_2O_3) [7], and barium sulfate ($BaSO_4$) [5]. $BaSO_4$ is a naturally occurring, non-toxic, and cost-effective material conventionally used in clinical applications [4]. Due to its safety and affordability, $BaSO_4$ is a promising alternative material for X-ray shielding [2]. Additionally, $BaSO_4$ has been incorporated into various composite materials, such as natural rubber [1-2, 4, 8], polydimethylsiloxane rubber [5],

EPDM rubber [3,9], and concrete [10]. Natural rubber (NR) foam composites offer several advantages, including high elasticity, elongation at break, tensile strength, and tear resistance. Therefore, NR/$BaSO_4$ foam composites provide flexibility, lightweight properties, fracture resistance, and high efficiency in radiation shielding [1].

In this study, lead-free X-ray shielding materials were prepared using NR/$BaSO_4$ foam composites with $BaSO_4$ filler loadings of 0-100 phr via the Dunlop method. This method is convenient, reliable, cost-effective, and energy-efficient. The study aimed to evaluate the effects of X-ray tube voltage (60-90 kVp) and material thickness on the X-ray shielding properties of the NR/$BaSO_4$ foam composites.

2. Materials and Methods

2.1 Materials

High-ammonia natural rubber (NR) latex with a 60% dry rubber content was obtained from the Center of Rubber Technology for Community, Faculty of Engineering, Thaksin University, Phatthalung, Thailand. Barium sulfate ($BaSO_4$) particles (0.3 μm) were purchased from Scitrader Co., Ltd., Thailand. The following chemicals were used as additives: sulfur (S), zinc diethyldithiocarbamate (ZDEC), zinc 2-mercaptobenzothiazole (ZMBT), Wingstay®-L, zinc oxide (ZnO), diphenyl guanidine (DPG), and sodium silicofluoride (SSF). These chemicals were acquired from VPK Supply Co., Ltd., Thailand, and were used in an aqueous dispersion form prepared in the laboratory.

2.2 Preparation of NR/$BaSO_4$ foam composites

All ingredients were compounded according to the formulation shown in Table 1 [11]. The NR latex and $BaSO_4$ powders were blended with the other ingredients using mechanical stirring. The resulting foam mixture was poured into a mold (25 × 25 × 0.5 cm^3). The NR/$BaSO_4$ foam was vulcanized at 100°C for 1 hour in an oven, following a fabrication process previously described [11].

Table 1. Material formulations for NR/$BaSO_4$ foam composites preparation [11].

Ingredients	Total solid content (%)	Dry weight (phr*)
HA latex	60	100
S	50	2
ZDEC	50	2.5
ZMBT	50	2
Wingstay® L	50	1
ZnO	50	5
DPG	40	2
SSF	20	0.5
$BaSO_4$ (phr)	0, 50,75, 100	

* phr is the ratio unit of weight part of chemicals to 100 wt parts of rubber

2.3 Characterizations

2.3.1 Morphological properties

The NR/$BaSO_4$ foam composite surface morphology was analyzed using a Scanning Electron Microscope (SEM: FEI, Quanta 450 FEG). SEM observations were conducted at a voltage of 5 kV. Before SEM examination, the dried foam samples were vacuum-coated with gold and palladium to enhance conductivity. For morphological analysis, images were captured from three different areas of each NR/$BaSO_4$ sample; however, only a representative image is presented.

2.3.2 Physical properties

The foaming characteristics of NR/$BaSO_4$ foam composites were analyzed based on expansion ratio (ER) and foam porosity (V_f). The expansion ratio reflects the capacity of cellular materials to expand in volume

during the foaming process. This parameter was determined by calculating the ratio between the density of solid NR (ρ_r = 0.93 g/cm^3) and that of NR/$BaSO_4$ foam composites (ρ_f), as described in equation (1) [12].

$$ER = \frac{\rho_r}{\rho_f} \tag{1}$$

Foam porosity, representing the proportion of void spaces within the foam structure, was evaluated using equation (2) [12].

$$V_f = \left(1 - \frac{\rho_f}{\rho_r}\right) \times 100 \tag{2}$$

2.3.3 X-Ray shielding properties

NR/$BaSO_4$ foam composite samples, measuring 3.5 cm × 3.5 cm, were positioned between an X-ray generator (MRAD-A32S, CANON) and an X-ray measuring instrument (X2, RAYSAFE). The samples, with thicknesses ranging from 0.5 cm to 2.5 cm, were exposed to a narrow X-ray beam at tube voltages of 60, 70, 80, and 90 kVp with a current of 200 mA. The exposure time was set to 0.05 seconds. The X-ray tube was placed at a fixed distance of 1 meter from the NR/$BaSO_4$ foam composites, as illustrated in Figure 1. The incident X-ray intensity (I_0) and the transmitted X-ray intensity (I) were recorded.

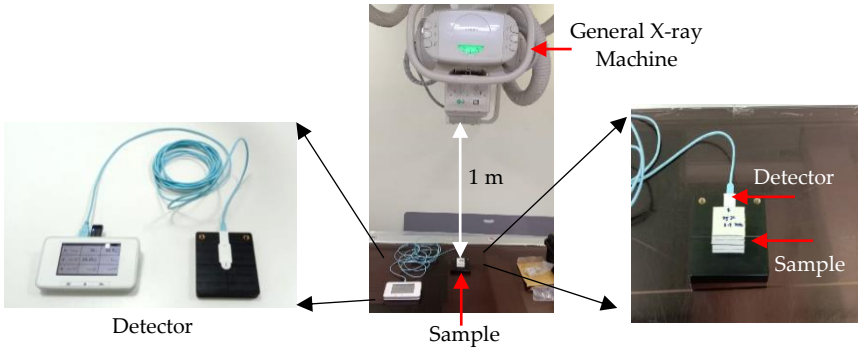

Figure 1. X-ray shielding property experiment setup.

The shielding properties of the NR/$BaSO_4$ foam composites were evaluated based on X-ray attenuation, linear attenuation coefficient (μ_l), mass attenuation coefficient (μ_m), and half-value layer (HVL). The X-ray attenuation efficiency was determined using the following equation (3) [12] :

$$X-ray\ attenuation = \frac{I_0 - I}{I_0} \times 100 \tag{3}$$

Where I and I_0 were the intensity of the transmitted X-ray and the intensity of the incident X-ray, respectively. The linear attenuation coefficients (μ_l) were calculated using the following equation (4) [12] :

$$I = I_0 e^{-\mu_l x} \tag{4}$$

$$ln\left(\frac{I_0}{I}\right) = \mu_l x \tag{5}$$

A plot of $\ln(I_0/I)$ versus thickness (x) was used to determine μ_l the slope of the trendline [8]. The mass attenuation coefficient (μ_m) was obtained using equation (6) :

$$\mu_m = \frac{\mu_l}{\rho} \tag{6}$$

Where ρ represents the density of the NR/$BaSO_4$ foam composites. The density values from a previous study [11] were used for these calculations.

The half-value layer (HVL), which refers to the thickness required to reduce the X-ray intensity by 50%, was determined using equation (7) [13,14] :

$$HVL = \frac{ln\,2}{\mu_l} \tag{7}$$

Table 2. The densities of NR/$BaSO_4$ foam composites with varying contents of $BaSO_4$ [11].

$BaSO_4$ content (phr)	0	50	75	100
Density (g/cm^3)	0.59 ± 0.02	0.61 ± 0.02	0.64 ± 0.01	0.70 ± 0.01

3. Results and Discussion

3.1 Morphological properties

Figure 2 presents SEM micrographs that reveal that increasing $BaSO_4$ content (0-100 phr) significantly alters the foam structure. At 0 phr, the foam exhibits a highly porous, uniform structure. At 50 phr, $BaSO_4$ particles are well dispersed, maintaining porosity with thicker cell walls. At 75 phr, pore size decreases, and slight agglomeration appears, affecting homogeneity. At 100 phr, severe particle agglomeration is observed, leading to a denser, less porous structure. While higher $BaSO_4$ loading improves X-ray shielding efficiency, excessive amounts lead to particle agglomeration, reduced foam expansion, and compromised mechanical properties.

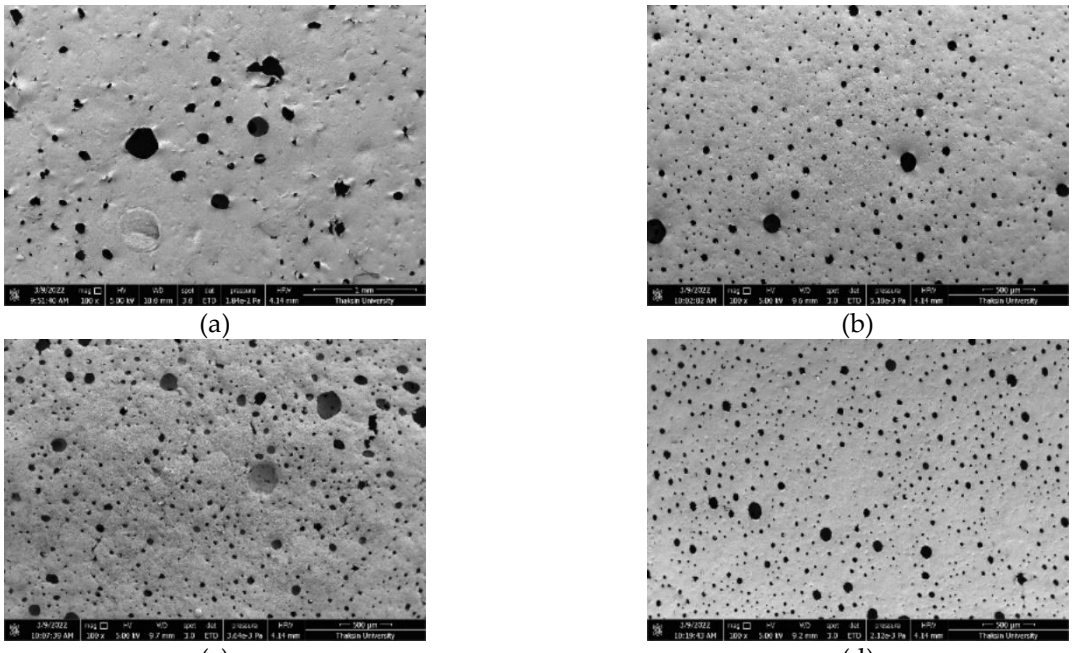

(a) (b) (c) (d)

Figure 2. SEM micrographs of NR/$BaSO_4$ foam composites at various $BaSO_4$ filler loadings : (a) 0 phr, (b) 50 phr, (c) 75 phr, and (d) 100 phr.

3.2 Physical properties

Figure 3 illustrates the expansion ratio (ER) and porosity (Vf) of NR/ $BaSO_4$ foam composites with increasing $BaSO_4$ content (0-100 phr). At 0 phr, the foam exhibits the highest ER and porosity, indicating a well-expanded structure. At 50 phr, ER and porosity slightly decrease but remain sufficient for maintaining flexibility. At 75 phr, both properties decline significantly, suggesting restricted foam expansion due to $BaSO_4$ particle interference. At 100 phr, severe reduction in ER and porosity is observed, leading to a denser, less porous structure. Excessive $BaSO_4$ hinders foam formation, reducing void spaces and increasing density.

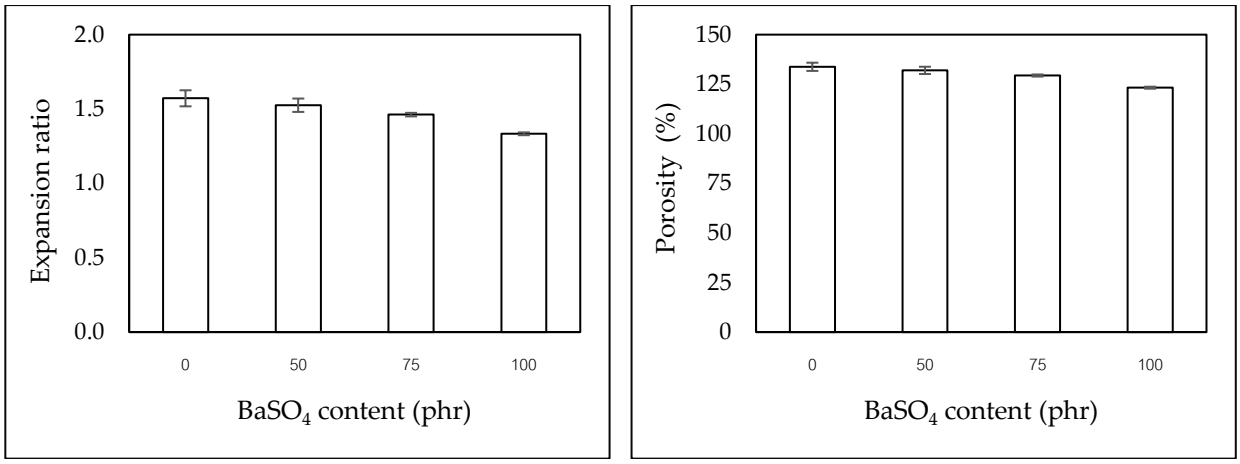

(a) (b)

Figure 3. Physical properties of NR/$BaSO_4$ foam composites at various $BaSO_4$ filler loadings : (a) Expansion ratio and (b) porosity

3.3 X-Ray shielding properties

Figure 4 illustrates the X-ray attenuation efficiency of NR/$BaSO_4$ foam composites as a function of $BaSO_4$ content and thickness at different X-ray tube voltages (60-90 kVp). The results show that X-ray attenuation increases with higher $BaSO_4$ content and greater material thickness. At 0 phr, attenuation is lowest, while at 100 phr, it is significantly improved due to the higher density of BaSO4. Increasing the voltage reduces attenuation efficiency since higher-energy X-rays penetrate more easily. Therefore, higher $BaSO_4$ loading enhances shielding effectiveness.

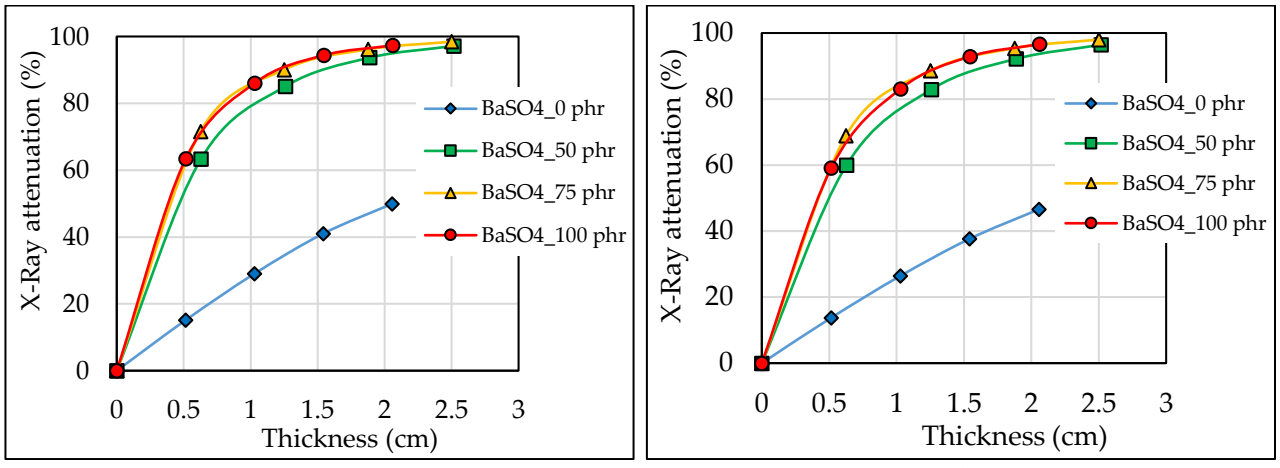

(a) (b)

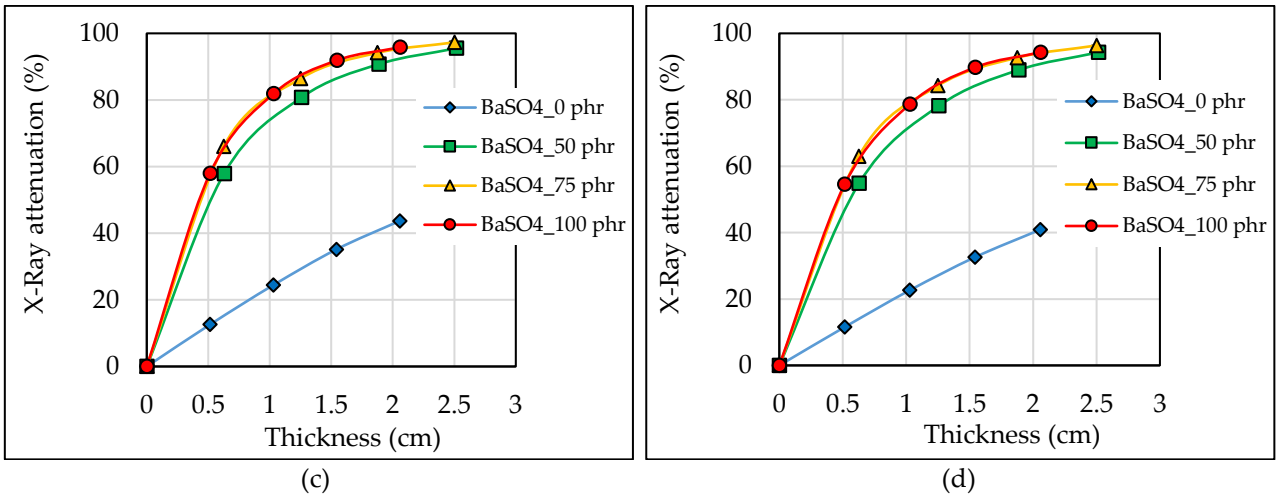

Figure 4. X-ray attenuation of NR/$BaSO_4$ foam composites as a function of thickness and $BaSO_4$ contents at different X-ray tube voltages. (a) 60 kV_P, (b) 70 kV_P, (c) 80 kV_P, and (d) 90 kV_P.

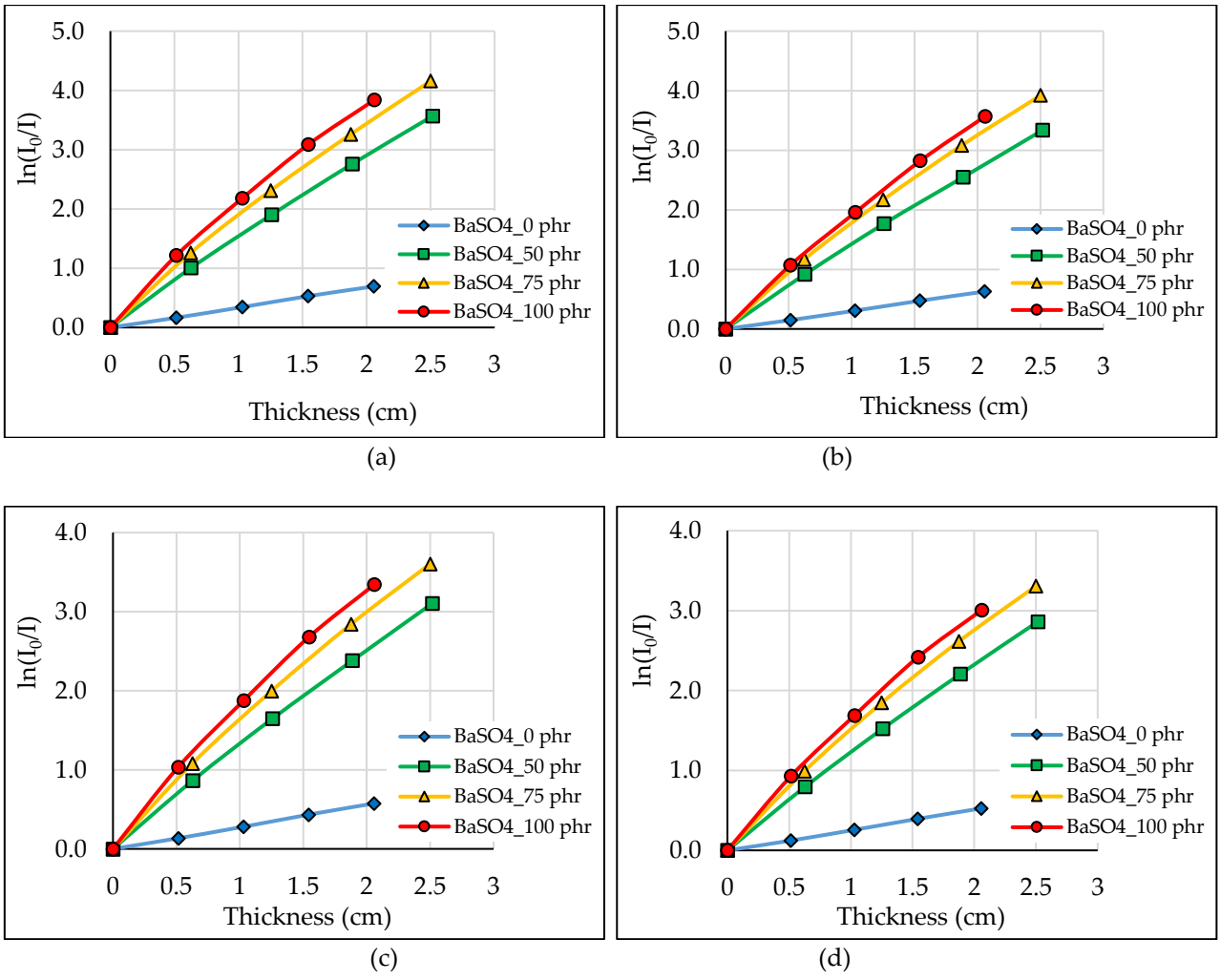

Figure 5. Graph of $ln(I_0 / I)$ as a function of thickness and $BaSO_4$ contents at different X-ray tube voltages. (a) 60 kV_P, (b) 70 kV_P, (c) 80 kV_P, and (d) 90 kV_P.

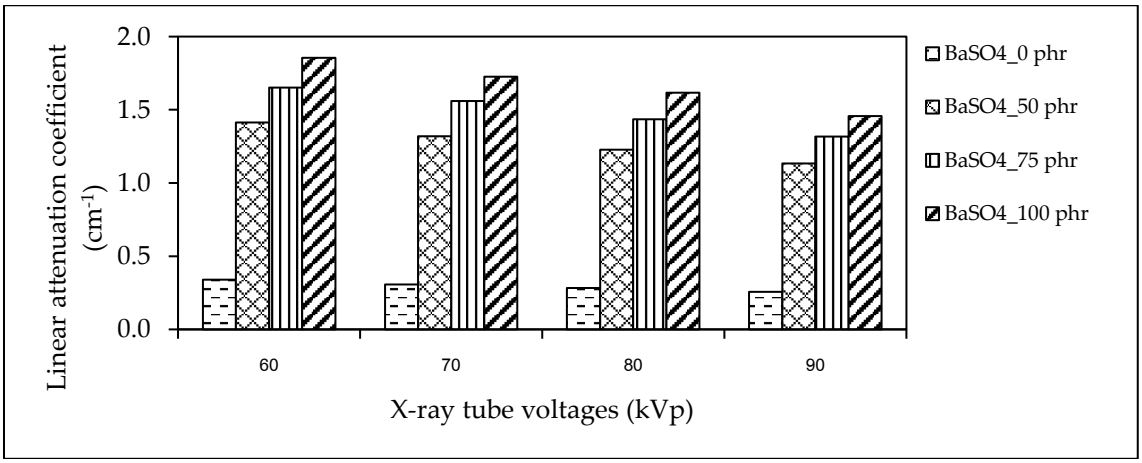

Figure 6. The linear attenuation coefficient of NR/$BaSO_4$ foam composites with different X-ray tube voltages.

Figure 7 illustrates the mass attenuation coefficient (μ_m) of NR/$BaSO_4$ foam composites at different X-ray tube voltages (60–90 kVp). The results show that μ_m it increases with higher $BaSO_4$ content, confirming that barium sulfate enhances X-ray absorption efficiency due to its high atomic number. However, μ_m it decreases as X-ray voltage increases, indicating that higher-energy X-rays penetrate the material more effectively, reducing attenuation. The trend aligns with expectations, showing that $BaSO_4$-enhanced composites are more effective at lower X-ray voltages, making them suitable for radiation shielding applications.

Figure 8 presents the half-value layer (HVL) of NR/$BaSO_4$ foam composites at different X-ray tube voltages. HVL represents the thickness required to reduce X-ray intensity by 50%, indicating the material's shielding efficiency. The results show that HVL decreases as $BaSO_4$ content increases, confirming that higher $BaSO_4$ loading enhances X-ray absorption, requiring less material thickness for effective attenuation. However, HVL increases with X-ray voltage, indicating that higher-energy X-rays penetrate more easily, reducing shielding efficiency.

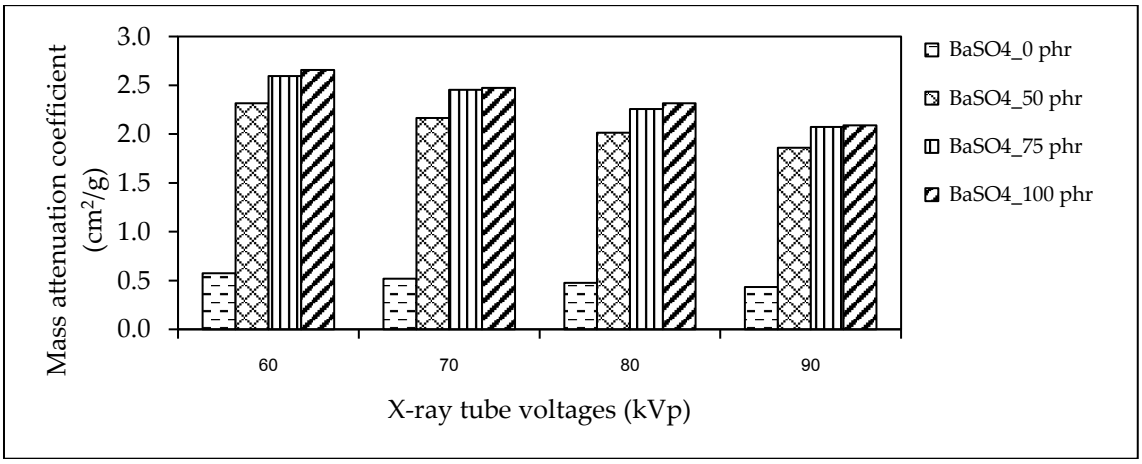

Figure 7. The mass attenuation coefficient of NR/$BaSO_4$ foam composites with different X-ray tube voltages.

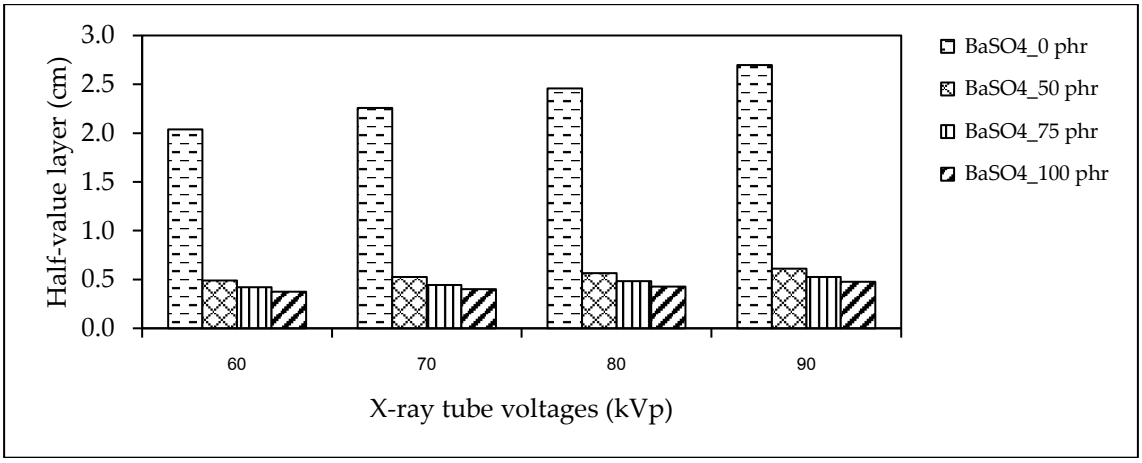

Figure 8. The half-value layer of NR/$BaSO_4$ foam composites with different X-ray tube voltages.

4. Conclusions

This study confirms that NR/$BaSO_4$ foam composites exhibit enhanced X-ray shielding efficiency with increasing $BaSO_4$ content. Higher $BaSO_4$ loading leads to reduced pore size and increased material density, affecting foam expansion and porosity. The addition of $BaSO_4$ significantly improves X-ray attenuation, with more excellent absorption observed at lower X-ray voltages. The linear and mass attenuation coefficients increase with $BaSO_4$ content, confirming enhanced radiation shielding capability. Conversely, the half-value layer decreases as $BaSO_4$ content rises, indicating better-shielding performance. However, at higher X-ray voltages, attenuation efficiency is reduced due to greater penetration. The results suggest that NR/$BaSO_4$ foam composites with 75–100 phr $BaSO_4$ provide an optimal balance between effective X-ray shielding and structural integrity, making them suitable for flexible, lead-free radiation protection materials.

5. Acknowledgements

This work was supported by the National Higher Education, Science, Research and Innovation Policy Council, Thaksin University (Research project grant), Fiscal Year 2022. The authors gratefully acknowledge the Center of Rubber Technology for Community, Faculty of Engineering, Thaksin University, Phatthalung, Thailand, and the Regional Medical Sciences Center 11, Suratthani, Thailand.

Author Contributions: Conceptualization, S. K. and A. S.; designed the experiments, S. K. and A. S.; performed the experiments, S. K., A. S., S. P. and N. K.; analysis and investigation, S. K. and P. B.; writing—review and editing, S. K. and P. B.; All authors have read and agreed to the published version of the manuscript."

Funding: This research was funded by the National Higher Education, Science, Research and Innovation Policy Council and Thaksin University (Research project grant) Fiscal Year 2022.

Conflicts of Interest: The authors declare no conflict of interest.

References

[1] Kalkornsurapranee, E.; Kothan, S.; Intom, S.; Johns, J.; Kaewjaeng, S.; Kedkaew, C.; Chaiphaksa, W.; Sareein, T.; Kaewkhao, J. Wearable and flexible radiation shielding natural rubber composites: Effect of different radiation shielding fillers. Radiat. *Phys. Chem*. **2021**, *179*, 1-8. https://doi.org/10.1016/j.radphyschem.2020.109261.

[2] Mungpayaban, H.; Rindhatayathon, P.; Ninlaphruk, S.; Rueanngoen, A.; Ekgasit, S.; Pengprecha, S. X-ray protective materials from barium sulfate/amorphous cellulose/natural rubber composites. *Radiat. Phys. Chem*. **2022**, *194*, 1-10. https://doi.org/10.1016/j.radphyschem.2022.110011.

[3] Poltabtim, W.; Wimolmala, E.; Saenboonruang, K. Properties of lead-free gamma-ray shielding materials from metal oxide/EPDM rubber composites. *Radiat. Phys. Chem*. **2018**, *153*, 1–9. https://doi.org/10.1016/j.radphyschem.2018.08.036

[4] Plangpleng, N.; Charoenphun, P.; Polpanich, D.; Sakulkaew, K.; Buasuwan, N.; Onjun, O.; Chuamsaamarkkee, K. Flexible gamma ray shielding based on natural Rubber/$BaSO_4$ nanocomposites. *Radiat. Phys. Chem*. **2022**, *199*, 1-8. https://doi.org/10.1016/j.radphyschem.2022.110311.

[5] Kumar, P.; Niranjana, P.T.; Jineesh, A.G. $BaSO_4$ and Fe_2O_3 Filled polydimethylsiloxane elastomer nanocomposite as x-ray radiation resistant material. *RUAS-SASTech J*. **2018**, *17(1)*, 1-4.

[6] Onjun, O.; Buasuwan, N.; Rungseesumran, T.; Kamwang, N.; Channuie, J. Natural rubber block as gamma radiation shielding for medical applications. *J. Phys. Conf. Ser 1285.* **2019**, 1-8. https://doi:10.1088/1742-6596/1285/1/012048.

[7] Poltabtim, W.; Wimolmala, E.; Markpin, T.; Sombatsompop, N.; Rosarpitak, V.; Saenboonruang, K. X-ray shielding, mechanical, physical, and water absorption properties of wood/PVC composites containing bismuth oxide. *Polymers*. **2021**, *13*, 1-16. https://doi.org/10.3390/polym13132212.

[8] Jaiyen, S.; Phumsuwan, A.; Thongpool, V.; Phunpueok, A. Determination of radiation attenuation coefficients of rubber containing barite. *Appl. Mech. Mater.* **2017**, *866,* 204-207. https://doi.org/10.4028/www.scientific.net/AMM.866.204.

[9] Cherkasov, V.; Yurkin, Y.; Avdinin, V.; Suntsov, D. Self-adhesion x-ray shielding composite material of EPDM rubber with barite: Mechanical Properties. *Mater. Plast.* **2020**, *57,* 28-36. https://doi.org/10.37358/MP.20.1.5309.

[10] Akkurt, I.; Akyıldırım, H.; Mavi, B.; Kilincarslan, S.; Basyigit, C. Photon attenuation coefficients of concrete includes barite in different rate. *Ann. Nucl. Energy.* **2010**, *37,* 910–914. https://doi.org/10.1016/j.anucene.2010.04.001.

[11] Konruang, S.; Srisook, A.; Buaphet, P.; Tayeh, F.; Naebpetch, W. Preparation of Lead-Free X-Ray Shielding materials based on Natural Rubber/Barium Sulfate composites. *ASEAN J. Sci. Technol. Rep.* **2022**, *25,* 59-66. https://doi.org/10.55164/ajstr.v25i2.246574

[12] Sukkaneewat, B.; Utara, S. Ultrasonic-assisted Dunlop method for natural rubber latex foam production: Effects of irradiation time on morphology and physico-mechanical properties of the foam. *Ultrason. Sonochem.* **2022**, *82*, https://doi.org/10.1016/j.ultsonch.2021.105873.